JACS
JOURNAL OF THE AMERICAN CHEMICAL SOCIETY

ARTICLE

pubs.acs.org/JACS

Evidence for Quantum Interference in SAMs of Arylethynylene Thiolates in Tunneling Junctions with Eutectic Ga−In (EGaIn) Top-Contacts

Davide Fracasso,[†] Hennie Valkenier,[†] Jan C. Hummelen,[†] Gemma C. Solomon,[*,‡] and Ryan C. Chiechi[*,†]

[†]Stratingh Institute for Chemistry and Zernike Institute for Advanced Materials, University of Groningen, Nijenborgh 4, 9747 AG Groningen, The Netherlands

[‡]Nano-Science Center and Department of Chemistry, University of Copenhagen, Universitetsparken 5, 2100 Copenhagen Ø, Denmark

Supporting Information

ABSTRACT: This paper compares the current density (J) versus applied bias (V) of self-assembled monolayers (SAMs) of three different ethynylthiophenol-functionalized anthracene derivatives of approximately the same thickness with linear-conjugation (AC), cross-conjugation (AQ), and broken-conjugation (AH) using liquid eutectic Ga−In (EGaIn) supporting a native skin (~1 nm thick) of Ga_2O_3 as a nondamaging, conformal top-contact. This skin imparts non-Newtonian rheological properties that distinguish EGaIn from other top-contacts; however, it may also have limited the maximum values of J observed for AC. The measured values of J for AH and AQ are not significantly different ($J \approx 10^{-1}$ A/cm^2 at $V = 0.4$ V). For AC, however, J is 1 (using log averages) or 2 (using Gaussian fits) orders of magnitude higher than for AH and AQ. These values are in good qualitative agreement with gDFTB calculations on single AC, AQ, and AH molecules chemisorbed between Au contacts that predict currents, I, that are 2 orders of magnitude higher for AC than for AH at $0 < |V| < 0.4$ V. The calculations predict a higher value of I for AQ than for AH; however, the magnitude is highly dependent on the position of the Fermi energy, which cannot be calculated precisely. In this sense, the theoretical predictions and experimental conclusions agree that linearly conjugated AC is significantly more conductive than either cross-conjugated AQ or broken conjugate AH and that AQ and AH cannot necessarily be easily differentiated from each other. These observations are ascribed to quantum interference effects. The agreement between the theoretical predictions on single molecules and the measurements on SAMs suggest that molecule−molecule interactions do not play a significant role in the transport properties of AC, AQ, and AH.

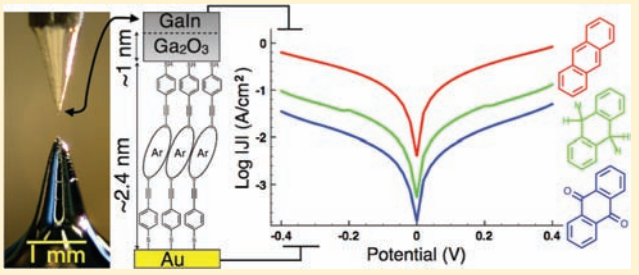

INTRODUCTION

This paper describes the measurement of current densities (J) through junctions comprising self-assembled monolayers (SAMs) of three arylethynylene thiolates (that differ only in their conjugation patterns) on Au substrates using eutectic Ga−In (EGaIn; 75% Ga, 25% In by weight, mp = 15.5 °C)[1] as a conformal top-contact. We compared the values of J at applied biases (V) between −0.4 and +0.4 V for these three different ethynylthiophenol-functionalized anthracene derivatives (Figure 1) with the predicted values from transport calculations (using gDFTB) for the molecules chemisorbed between two gold electrodes. We predicted and observed a dramatic reduction in J where destructive quantum interference effects dominate the transport properties. Although we do not expect quantitative agreement, we find good qualitative agreement between experiment and theory; the linear-conjugation of the anthracene core is at least 10 times more conductive than the broken-conjugation and cross-conjugation of the 9,10-dihydroanthracene and 9,10-anthraquionone cores. To the best of our knowledge, this is the first report of the measurement of unsaturated molecules using EGaIn and the first experimental study of the influence of cross-conjugation on J in junctions containing a SAM.

Cross-Conjugation and Quantum Interference Effects. Chemistry is replete with cases where seemingly minor changes in the chemical structure of a molecule result in significant changes in a physical property of the system. In conjugated molecules, there are particular relationships between parts of the molecule that govern a whole range of the physical and chemical properties. For example, the substitution patterns of benzene derivatives are well-established; electrophiles prefer to add *ortho* or *para* to electron-rich substituents. This effect is amplified for substituents with a lone pair because of the resonance structures that place negative charges *ortho* and *para* to the substituent. Another way to look at these substitution patterns, and the reason there are no resonance contributors with negative charges on the *meta* positions, is that the *ortho* and *para* positions are linearly conjugated, whereas the *meta* position is cross-conjugated (with respect to the substituent).

Received: March 18, 2011
Published: May 11, 2011

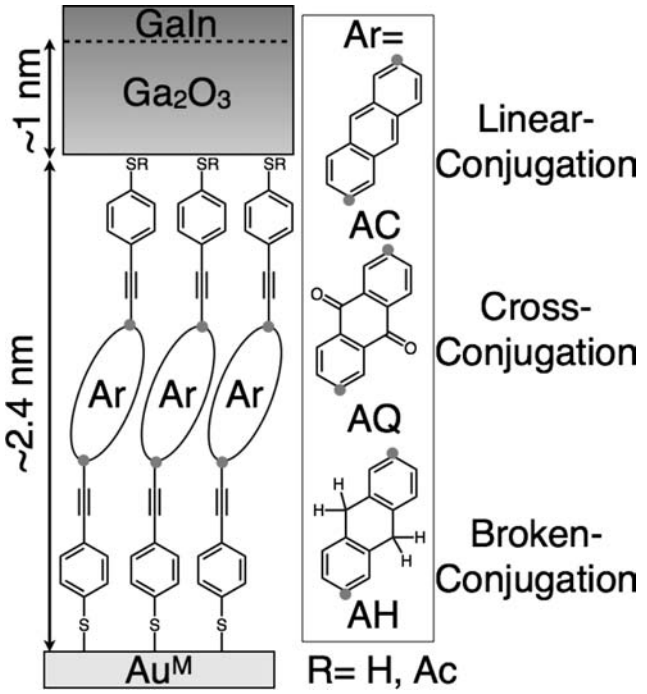

Figure 1. Schematic of the tunneling junctions (not to scale) of gold-on-mica supporting SAMs of thiolated arylethynylenes with cores of anthracene (AC; linear-conjugation), 9,10-anthraquinone (AQ; cross-conjugation), or 9,10-dihydroanthracene (AH; broken-conjugation) connected at the 2,6 positions (indicated with gray circles). The thiolate groups at the GaIn|Ga_2O_3 interface comprise a random mixture of free thiols and thioacetates.

Thus, although the *meta* position is in the same π circuit and one carbon atom away from either the *ortho* or *para* positions, there is no resonance structure that places the lone pair of a substituent on the *meta* position of the benzene ring. A dramatic example of this phenomenon of cross-conjugation, i.e., atoms connected by a continuous circuit of p orbitals in which there is no resonance structure that places alternating double and single bonds between them,[2] can be seen in conjugated polymers where cross-conjugating ketones in the backbone produce an apparently conjugated polymer that is pale yellow (it has a large optical band gap). Reducing these ketones electrochemically (in the solid state) produces a linearly conjugated π-system and the bulk absorption shifts from the near-UV (pale yellow) to the near-IR (purple-gray).[3]

The ability to control the flow of charge at the *quantum* level through organic synthesis is a tantalizing prospect that draws researchers from myriad subdisciplines of chemistry and physics to molecular electronics (ME). In this context conjugation is a powerful but relatively simple synthetic handle; cross-conjugation results in transport properties that are dramatically different from those observed in linearly conjugated systems. The propensity for a molecule to conduct electrical current is related to the same underlying physical processes that determine the types of resonance structures that are permitted for the molecule; however, electrical current due to a tunneling process need not be described by single charges hopping through a molecule. Cross-conjugation, whether it be through *meta* substitution on a benzene ring[4−17] or other cyclic[18,19] or acyclic[20,21] structures, results in significantly reduced electron transport, as destructive interference effects can dominate the low-bias current. Theoretical models predict that this effect extends to anthracene systems.[22] For these molecules, instead of having to alter the connectivity to the aromatic system, conjugation can be controlled by chemically modifying the anthracene moieties, for example, via redox switching between anthraquinone and anthrahydroquinone.[19,23] Recently, the effect of quantum interference was observed for photoinduced electron transfer across linearly conjugated and cross-conjugated acyclic bridges,[24] but to the best of our knowledge, there are only two observations of the influence of cross-conjugation in tunneling junctions, both of which concluding only that *meta* contacts lead to less current passing through a single-molecule junction compared with *para* contacts.[16,17] Another study observed a decrease in the conductance of single-molecule junctions that are photochemically switched between linearly conjugated and cross-conjugated states; however, the authors did not ascribe this effect to cross-conjugation or quantum interference.[25]

Tunneling Junctions Comprising SAMs. A central challenge for ME remains the formation of electrical contacts to molecules that allow the measurement of current through individual molecules, i.e., molecular junctions.[26,27] There are two strategies for forming these junctions: defining the smallest dimension using the molecules (i.e., bottom-up) or preforming a molecule-sized gap and populating it with the molecules (i.e., top-down). The former strategy utilizes a top-contact that is placed on top of preformed SAM, whereas the latter is almost exclusively used for single-molecule measurements, which are not easily comparable to SAM-based measurements comprising micrometer-sized areas of molecules. Two notable exceptions are CP-AFM,[28,29] in which a conductive AFM tip is brought into contact with a SAM, and STM break-junctions[30,31] (STM-BJs), in which molecules are plucked from a monolayer of dithiolates using a Au STM tip. These methods form the smallest dimension through the placement of the probe tip but ostensibly use the length of the molecules to define this dimension. They are, however, clearly top-down,[32] and whereas CP-AFM may be considered a SAM-based (or few-molecule) measurement, STM-BJs are single-molecule measurements. We form a probe of EGaIn that is ~25 μm in diameter, position it laterally with an adjustable stage, and bring it into contact with a SAM using a piezo stepper (open-loop, ~5 nm resolution). Unlike with other probe techniques, EGaIn is a liquid at room temperature, and therefore, owing to the mechanical stability of densely packed SAMs, it makes a conformal contact to the surface of the SAM; it is a bottom-up technique. Though EGaIn is similar to the Hg-drop method,[33−39] in that it uses a liquid metal as a top-contact, the rheological properties of EGaIn[40] allow it to retain conical shapes in the liquid phase. This shear-yielding behavior (i.e., below critical values of surface shear stress EGaIn does not flow) is driven by the spontaneous formation of a self-limiting layer of Ga_2O_3 at the EGaIn/air interface.[41] The oxide layer obviates the need for a solvent bath and a second monolayer on the liquid metal electrode (both of which are usually required for Hg-drop measurements), and thus measurements can be performed by directly contacting EGaIn to a SAM under ambient conditions. EGaIn tips can also be used to measure several junctions or regenerated on the same substrate that is being measured, whereas Hg tends to amalgamate with the metal substrate after a few scans. Thus EGaIn resembles a scanning-probe technique more than a hanging-drop technique, but with six key advantages: (i) it forms micrometer-sized contacts of reproducible size that can be resolved optically and which produce relatively large currents (nA−mA), (ii) the experimental setup is exceedingly simple, (iii) measurements are performed under

ambient conditions, (iv) junctions are formed rapidly, which allows large data sets to be quickly collected across various substrates, (v) it is compatible with microfluidics,[40,42,43] and (vi) the junctions are readily disassembled after measurement, allowing the SAM to be inspected *post facto*. The principal advantage of EGaIn, however, is its overall simplicity; it requires very little training and no specialized equipment, and the interpretation of the data is straightforward.[44] It is therefore accessible to chemists as a potential "benchtop" tool for rapidly screening the transport properties of organic structures or performing basic physical-organic studies. (For a more rigorous comparison of EGaIn with other methods for contacting molecules refer to Nijhuis et al.[45])

Although EGaIn is a relatively new tool for ME,[46] it has been used to measure molecular junctions comprising simple alkanes as well as ferrocene-terminated alkanes that exhibit temperature-dependent[42] molecular rectification.[45] These studies focused on the length-dependence of alkanes, determining the characteristic decay constant, β, from $J = J_0\, e^{-\beta d}$ (where d is the thickness and J_0 is the theoretical current at $d = 0$) and the interfaces; observing rectification behavior of ferrocene-terminated SAMs. We are interested in using EGaIn to explore the influence of the electronic structure of conjugated molecules on the transport properties of SAMs. The challenge in performing this type of study on SAMs is altering the electronic properties without perturbing the thickness of the SAM. One approach utilizes the commensurate change in effective conjugation as a function of torsional angle in oligo(*p*-phenylene) derivatives.[47] We chose phenylethynylene-substituted anthracene moieties because the electronic structure can be manipulated synthetically with relatively minor perturbations to the molecules and the subsequent SAMs (in particular, the thickness). The manipulation of the central aromatic ring (by substitutions at the 9 and 10 positions of the anthracene) allows the direct comparison of different conjugated pathways through the same molecular framework. We measured three different anthracene derivatives (the syntheses of which are described elsewhere[23,48]) functionalized at the 2,6 positions with *p*-ethynylthiophenols: (i) anthracene (AC), which is linearly conjugated, (ii) anthraquinone (AQ), which is cross-conjugated, and (iii) dihydroanthracene (AH), in which the conjugation is broken (Figure 1).

RESULTS AND DISCUSSION

Nomenclature. We denote the type of substrate using the atomic symbol of the metal with a superscript indicating how it was prepared: M for mica and TS for template-stripped. We describe the configuration of junctions using "/" to denote chemisorbed species, "//" to denote physisorbed contacts, and "|" to denote the interface between EGaIn and Ga_2O_3. Thus "EGaIn|Ga_2O_3//$CH_3(CH_2)_{11}S$/Au^{TS}" would denote a junction comprising a SAM of dodecanethiolate formed on a template-stripped gold substrate with a van der Waals contact between the terminal methyl group and the native oxide of the EGaIn top-contact. We refer to one J/V cycle, $0\,V \rightarrow +V_{max} \rightarrow -V_{max} \rightarrow 0\,V$ as a "trace." We use the terms "conductive" and "conductance" advisedly in the context of SAMs, referring to the current that results from the tunneling probability; we assume that the currents from the SAMs reported in this paper (20−25 Å thick) are dominated by nonresonant, coherent tunneling.

EGaIn|Ga_2O_3//SAM/Au Junctions. A common feature of conformal top-contacts for SAMs is a buffer layer between the electrode and the SAM. In Hg-drop measurements this buffer layer is a second SAM[35] or an undoped conjugated polymer.[49] In LAMJs this buffer layer is PEDOT:PSS.[50,51] For EGaIn the native Ga_2O_3 skin effectively serves the same function as a buffer layer. The term J_0, obtained from the *y*-intercept of plots of ln J versus d, is a combination of the conductivity of the buffer layer and the interfaces with the electrode and substrate (i.e., J in the absence of the physical separation of the electrodes by the SAM). Comparisons of tunneling in Hg-drops in three-electrode electrochemical measurements on SAMs of alkanethiolates reveal two values for J_0: with and without a second SAM acting as a buffer layer on the top Hg electrode.[38] The influence of PEDOT:PSS on J_0 has been studied in more detail[52] and it appears that the conductivity of PEDOT:PSS (the buffer layer) strongly influences J_0 and therefore limits the conductivity of the molecules that can be measured.[51] The conductivity of Ga_2O_3 has been measured;[53] however, it is difficult to correlate these values directly to EGaIn junctions. One study estimated the resistivity of EGaIn|Ga_2O_3 contacted to copper wires to be 0.04 Ω/cm^2, which corresponds to a maximum J at 0.2 V of 5.5 A/cm^2.[45] A related study showed that EGaIn junctions are sensitive to the energies of the orbitals present at the EGaIn|Ga_2O_3//SAM interface, indicating that the voltage drops across the entire junction (including the SAM) and not only at the Ga_2O_3 layer.[54] Extrapolations of many different data sets from Ag-SAM//Ga_2O_3|EGaIn junctions of alkanethiolates yield values of J_0 between 10 and 10^4 A/cm^2 for methyl-terminated alkanthiolates.[44] Thus, it is likely that the conductivity of the Ga_2O_3 buffer layer strongly influences J_0 and therefore also limits the conductivity of the molecules that can be measured. This limit is inconsequential for SAMs of alkanethiolates because alkanethiols that are short enough to exceed 10 A/cm^2 do not form ordered monolayers. For SAMs of conjugated molecules, however, we must be cautious of this potential upper limit of the conductivities of the molecules that can be measured using EGaIn.

All of the previous measurements using EGaIn were done using template-stripped[55] Ag surfaces (Ag^{TS}) as the substrate for the SAM. These ultrasmooth surfaces are extremely simple to prepare and dramatically reduce the influence of substrate-induced defects in the SAM on J.[56] Although using Ag^{TS} does not completely prevent shorts, it increases the yield of non-shorted junctions to >95% (for methyl- and ferrocene-terminated alkanethiolates), allowing all of the data, including shorts and abnormally low "no-contact" J/V traces, to be used to construct histograms of log|J| for each V. These histograms are normally distributed because J depends exponentially on randomly distributed variables (defects) and thus varies log-normal.[44−46,56,57] Fitting a Gaussian function yields a value of log|J| (the mean, μ_{log}) and error (from the standard deviation, $\pm \sigma_{log}$). These substrates, however, are supported by a photocured adhesive that is not compatible with the organic solvents required to dissolve the thioester precursors of AC, AQ, and AH. Thus, we formed SAMs on freshly prepared, thermally evaporated gold-on-mica (Au^M).[58,59] While Au^M consists of large islands of atomically flat Au(111), these islands are separated by large step-edges and crevices that function as defects and that are absent in Ag^{TS} surfaces. Coupled with the relative fragility of the SAMs of AC, AQ, and AH (compared to alkanethiolates) and the possibility that numerous J/V cycles can induce chemical reactions (i.e., dimerization of AC, redox of AQ, or elimination of H_2 from AH), we measure fewer scans per junction (six total; see

Experimental in the Supporting Information) and encounter a higher percentage of junctions that immediately short (20−30%). Of the junctions that do not immediately short, we also observe lower yields of junctions that do not short during measurement (∼80%) and broader distributions of log|J| than for junctions of EGaIn|Ga_2O_3//$CH_3(CH_2)_n$S/Au^{TS}. Using a piezo stepper to lower the EGaIn tip to the surface (instead of doing it by hand with a micromanipulator) enables us to measure these more fragile SAMs but also introduces more low-J, hysteretic "no-contact" traces. We therefore use an algorithm to filter these traces by defining shorts as I/V curves where $I > 10$ mA ($J \approx 10^3$A/cm^2) at 0.2 V and no-contact traces where $J \neq 0$ at 0 V, or in which dI/dV changes sign five or more times during a forward or reverse trace (the trace is noisy).[60] In general, the shape of a no-contact trace is the same as a trace generated with a visible gap between the EGaIn tip and the SAM, except that the magnitude of I is similar to when the tip is in contact. We therefore assume these traces to be the result of the EGaIn tip not physically contacting the SAM but being too close to visualize the gap between them. A junction that shorts either immediately or after several scans will often result in a filament of EGaIn between the SAM and the tip as it is moved away from the SAM, that is, shorts are most likely caused by the EGaIn penetrating the SAM and contacting the Au^M substrate. The net effect of all of these factors is that it is much more difficult to collect large data sets for AC, AQ, and AH than it is for alkanthiolates. The variance ($\sigma^2_{\log}$) of the histograms of log|J| is also roughly doubled, ∼0.25−0.5 log|A/cm^2| for alkanethiolates compared with ∼0.5−1.0 log|A/cm^2| for AC, AQ, and AH.

Measurement and Data Analysis. We initially prepared two substrates each for AC, AH, and AQ using Et_3N to deprotect the thioacetates *in situ* to form SAMs. Using a combination of ellipsometry and XPS we measured the thicknesses of the SAMs and found 25.1 Å for AC, 24.3 Å for AQ, and 19.0 Å for AH (see Supporting Information). The predicted (B3LYP/6-311g**) S−S distances are 24.5, 24.5, and 24.6 Å for AC, AQ, and AH respectively. (The bent form of AH that differs in energy by only 2.04 kcal/mol is 23.8 Å; see below.) These measured values predict, on the basis of thickness, the order of conductivities to be AH > AQ > AC, while the minimized values predict no observable difference. We did not observe either trend, and thus we conclude that the measured values of J are not dominated by length-dependence. Our chosen method of preparing SAMs of conjugated molecules produces dense monolayers but leaves a mixture of free thiols and thioacetates at the SAM//Ga_2O_3| EGaIn interface. (The procedure for forming and measuring the thicknesses of SAMs of conjugated thiolates is presented in detail elsewhere.[61]) It is possible that one of these head-groups electronically couples more tightly to the EGaIn|Ga_2O_3 and thus carries the majority of the current. The practical consequence of this is that we would underestimate J because not all of the molecules in the junction are contributing to the measured current. However, since all of the SAMs are prepared identically, the error would be systematic and would therefore not affect the comparison between the SAMs. We measured each substrate by recording five complete traces on each of 20−40 junctions on each substrate yielding roughly 100 traces per substrate (for a total of ∼200 traces each for AC, AQ, and AH) after discarding the shorts and no-contact traces. We computed J by measuring the width of the junctions using a calibrated on-screen ruler and assuming that the junctions were circular. We then computed the geometric average, $\overline{J}$, for each value of V and the standard error of the mean, SEM.[56] We initially chose to use the geometric average because the relatively low number (typical numbers for alkanethiolates are >1000) of traces makes it difficult to fit Gaussians using least-squares fitting algorithms, resulting in distorted line shapes of the resulting traces. (Also, although more complex statistical analyses are available,[57] their use is not necessary to understand our data and undermines the simple and straightforward nature of EGaIn measurements; see Supporting Information for a more detailed discussion of the statistical methods.) Typically log|$\overline{J}$| and SEM are good approximations of $\mu_{\log}$ and $\sigma_{\log}$, particularly with smaller data sets such as these. We computed the rectification ratio, R, for each value of $|V|$ from each trace and then computed the arithmetic mean (R is not normal or log-normal distributed), $\overline{R}$. These data are summarized in Figure 2. Junctions of EGaIn|Ga_2O_3//$CH_3(CH_2)_n$S/Ag^{TS} give $1.0 < \overline{R} < 1.5$, and we expect the same for AC, AQ, and AH because the molecules are symmetrical, but the interfaces with the electrodes are not. (Thus the voltage drop across the EGaIn|Ga_2O_3//SAM interface is greater than the S/Au^M interface.) The work function of EGaIn is about −4.3 eV, which is in between Au (−5.1 eV) and Ag (−4.7 eV), and thus we do not expect a large change in $\overline{R}$ moving from Ag^{TS} to Au^M substrates. We found $1.3 < \overline{R} < 1.5$ for AC, AQ, and AH, supporting the hypothesis that the current that we measure is the result of tunneling through the SAMs and not an artifact of the EGaIn|Ga_2O_3//SAM interface. (Typically this hypothesis is verified for a particular set of molecules by computing β, but that is not possible with three SAMs of equal thickness.) These values also rule out the influence of electrochemical processes such as the decarboxylation of the residual SAc groups, which would manifest as a significantly larger value for $\overline{R}$ because these processes take place only at one bias.

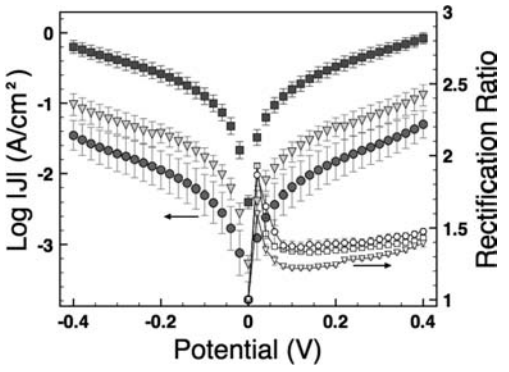

Figure 2. Left axis: plots of the geometric mean of log|J| versus V for AC (■), AQ (●), AH (▼). Error bars represent the standard error. Right axis: plots of the rectification ratios for AC (□), AQ (○), and AH (▽) versus $|V|$ computed from the arithmetic mean of $J(+V)/J(-V)$ for each trace. Error bars are computed from the standard error, SEM. These data show that AC (linear-conjugation) is at least 1 order of magnitude more conductive than AH (broken-conjugation) and AQ (cross-conjugation) while AH is slightly more conductive than AQ, though in some places the error bars overlap and thus we cannot conclude that they differ significantly from each other.

The geometric-averaged J/V data for AC, AH, and AQ show two trends: (i) J is at least 10 times higher for AC than for AQ or AH, and (ii) the error increases with decreasing J. The latter trend is most likely because the instrument is less accurate at low currents (10^{-2} A/cm$^2 \approx$ 100 nA), and thus the instrument error is superimposed on the distribution of J that is intrinsic to the

dx.doi.org/10.1021/ja202471m |*J. Am. Chem. Soc.* 2011, 133, 9556–9563

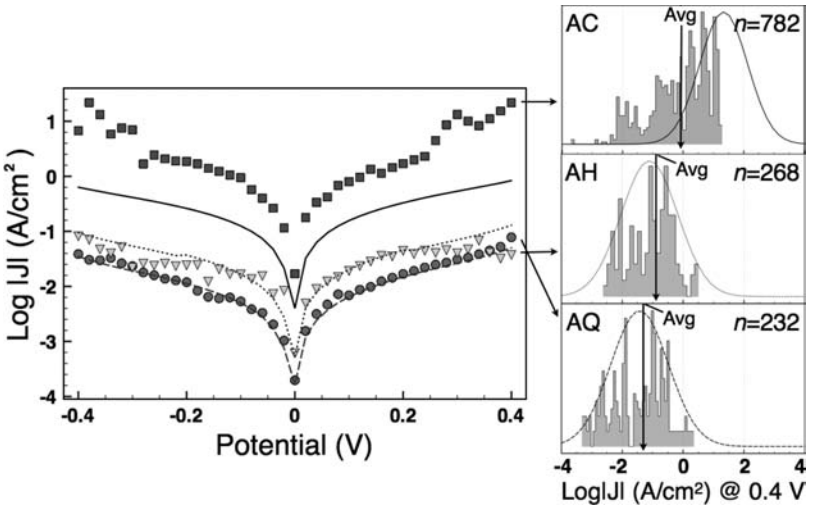

Figure 3. Left: plots of the geometric mean (lines) and Gaussian (μ_{log}) mean (symbols) of log|*J*| versus *V* for AC (solid line; ■), AH (dotted line; ▼), and AQ (dashed line; ●). Right: plots of the normalized histograms of log|*J*| at 0.4 V and the Gaussian fits for AC (top; solid line), AH (center; dotted line), and AQ (bottom; dashed line). The value of the geometric mean of log|*J*| is indicated with a solid arrow, and *n* is the total number of traces. These data reveal no appreciable difference between the geometric and Gaussian means for AH and AQ and clearly show that we cannot make a meaningful distinction between AH and AQ. The data for AC, however, form a truncated Gaussian distribution such that the Gaussian mean is more than an order or magnitude higher than the geometric mean. In either case, AC is clearly more conductive than either AH or AQ.

SAM. The former trend suggests that the linear-conjugation of AC makes it more conductive than the broken-conjugation of AH and the cross-conjugation of AQ. We ascribe this result to the fact that although both AC and AQ provide a continuous pathway of p orbitals (sp^2 and sp carbons between the S anchors) from EGaIn|Ga_2O_3 to Au^M, because the p orbitals in the center of the AQ belong to the orthogonal π bonds of the carbonyls, they comprise a cross-conjugated pathway between the electrodes. (These orthogonal bonds are, however, part of a carbonyl, which contains an electronegative oxygen atom, thus we cannot say that the *only* difference between AC and AQ is cross-conjugation.)

Despite the relatively low number of traces, to gain more insight into this finding we fit the histograms of log|*J*| for AC, AQ, and AH for each value of *V* to a Gaussian function (see Experimental in the Supporting Information) and plotted μ_{log} versus *V*. These data are plotted together with log|$\overline{J}$| in Figure 3 (the error bars representing the variance are omitted for clarity, $\sigma^2_{log} \approx 1$ log|A/cm^2| for AC, AQ, and AH); The histograms of log|*J*| at *V* = 0.4 V are shown to the right of the *J*/*V* traces. These fits show the expected agreement between log|$\overline{J}$| and μ_{log} for AH and AQ, as well as the distorted line shapes induced by the low number of traces. The *J*/*V* traces derived from the values of μ_{log} clearly show that the experiment cannot discern a statistically significant difference between AH and AQ. The data for AC differ greatly between the geometric average and Gaussian fits, with the latter giving values of *J* that about 1 order of magnitude higher. The reason for this discrepancy can be seen in the histogram for AC at *V* = 0.4 V. The data form a truncated Gaussian, the fit for which predicts values of μ_{log} that are about 1 order of magnitude higher than log|$\overline{J}$| (and are higher even than the maximum measured value of *J*). To address this discrepancy, we measured AC twice more (two substrates each, on two separate days, several weeks later, from freshly prepared Au^M and solutions of AC), and the resulting histogram did not change apart from the total number of counts; log|$\overline{J}$| did not change, nor did μ_{log}. These results suggest that this histogram reflects the tunneling properties of AC, which are converging on μ_{log}. We hypothesize that the data are being truncated by J_0 for this system, which means that although the peak conductance of AC is very close to that of the EGaIn|Ga_2O_3//AC interface, we are still able to observe it by virtue of the fact that the data are distributed log-normal. This cropping is evident through the entire range of *V* (though it is less obvious at *V* < 0.2 V; see Supporting Information). The values of log|$\overline{J}$|, which agree very well with those of μ_{log} for AQ and AH, diverge for AC because they are weighted by the lack of high values of *J*. Nevertheless, both the geometric average and Gaussian data clearly show that AC is more conductive than either AH or AQ. The only ambiguity is the magnitude of this difference: geometric-averaged values of *J* for AC are ~10 A/cm^2 larger than AH and AQ, whereas Gaussian-derived values of *J* are ~10^2 A/cm^2 larger.

Transport Calculations. Assuming coherent tunneling dominates the transport through the SAMs and that the *J*/*V* properties of the SAM are effectively the sum of the *I*/*V* properties of the individual molecules in a given area, it is natural to make a qualitative comparison of the EGaIn results with transport calculations on individual molecules. The atomic structure of the SAM//Ga_2O_3|EGaIn interface is unknown, so the problem is further simplified by considering the individual molecules chemisorbed between two Au electrodes. We optimized the isolated AC, AQ, and AH molecules (with terminal thiol groups) using Qchem[62] (DFT, B3LYP/6-311g**) and then chemisorbed them on the FCC hollow sites of two Au electrodes with a binding distance taken from the literature (Figure 4).[63] The minimized structure for AH is a bent conformation 2.04 kcal/mol lower in energy than the planar conformation. We included both conformations in the transport calculations as this energy difference indicates both conformations would be present at room temperature and we cannot predict which is dominant in the SAM. We calculated the transport using gDFTB[64−68] with no gold atoms included in the extended molecule. We integrated the bias-dependent transmission through the system over an energy window, the size of which is controlled by the magnitude of the

dx.doi.org/10.1021/ja202471m |*J. Am. Chem. Soc.* 2011, 133, 9556–9563

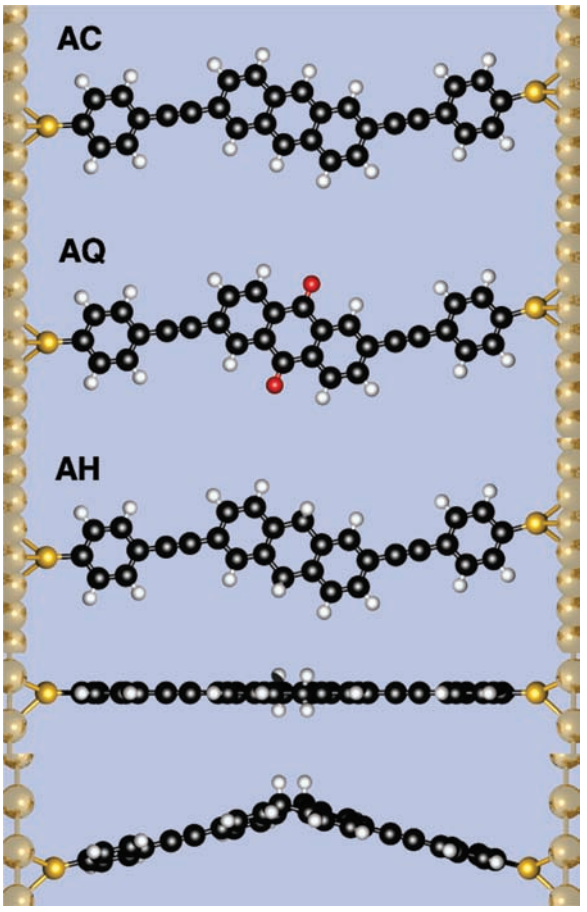

Figure 4. Minimized geometries of the three molecules AC, AQ, and AH used in the transport calculations. Two conformations (bottom) for AH were considered in order to take into account some of the conformational flexibility in this molecule at ambient temperature. In each case the molecules are chemisorbed at an FCC hollow site on each gold electrode.

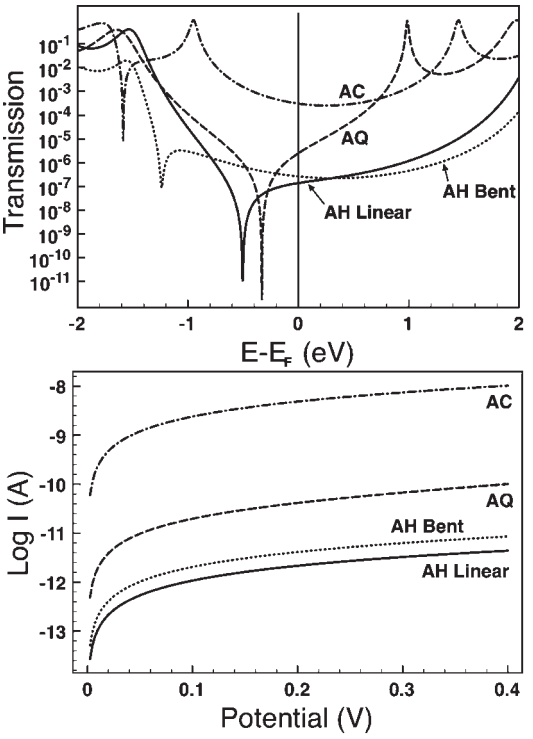

Figure 5. Transmission as a function of energy (top) and current as a function of voltage (bottom) for the three systems AC, AQ, and AH in the linear conformation and AH in the bent conformation, shown as dot-dash, dashed, solid, and dotted lines, respectively. The currents were calculated by integrating the transmission over increasing windows of bias.

applied bias, in order to obtain the current through the system. As the molecules are symmetrically bound to the two electrodes in the transport calculations, we assume that the applied bias drops symmetrically across the junction, a further point of departure from the measured EGaIn system. Although transmission is not an experimental observable, it shows the features that control the magnitude of the current through the molecules, and thus we plot both transmission and predicted I/V curves. These results are shown in Figure 5, clearly reproducing the experimental finding that AC is significantly more conductive than AQ or either conformation of AH. We plot transmission versus energy relative to the Au Fermi energy (here set to −5.0 eV), and interference features are evident slightly below the Fermi energy in the transmission through both AQ and the planar conformation of AH. The interference feature in the bent conformation of AH shifts to lower energy; however, this only results in a small change in the transmission near the Fermi energy. Conversely, there are no interference features evident in the off-resonant transmission near the Fermi energy for AC, and consequently this system exhibits transmission and current that are orders of magnitude higher than that of AQ and AH. It is interesting to note that the transport through the bent conformation of AH is actually higher than that through the planar conformation. The opposite trend would generally be expected for a predominantly conjugated molecule because deviations from planarity decrease electronic coupling. For AH, however, modulating the σ/hyperconjugative coupling with bending has a different effect and evidently the same "rules of thumb" do not apply. In any case, the difference between the two conformations is minimal. The transport calculations appear to suggest that the magnitude of the current through AQ and AH should be clearly distinguishable, with AQ exhibiting higher levels of transport and thus higher measured values of J. There is an important caveat to this result: the correct Fermi energy is an unknowable parameter in these calculations and there is undoubtedly a degree of uncertainty in its position. In cases such as these, where interference features mean the transmission varies significantly with even modest variations in the injection energy, the position of the Fermi energy can have a significant impact on the magnitude of the predicted I/V curves. Specifically, if the Fermi energy is effectively overestimated in these calculations then the difference between AQ and AH may also be overestimated. Conversely, if the Fermi energy is underestimated so too the difference between AQ and AH may be underestimated. In this sense, the calculations and experiment are in agreement: AC is more conductive than AH and AQ, but the differences between AQ and AH cannot necessarily be resolved. The predicted difference between AC and AQ (i.e., between the most and least conductive molecules) is 10^2, which agrees perfectly with the values of J derived from the Gaussian fits (Figure 3) but is 1 order of magnitude larger than the geometric-average values of J. While care must be exercised when comparing these theoretical predictions to experimental data, this result

dx.doi.org/10.1021/ja202471m |*J. Am. Chem. Soc.* 2011, 133, 9556–9563

strengthens the hypothesis that the Gaussian fits for the truncated histograms of log|J| are indeed correct in that they reflect the physical and electronic properties of AC.

The qualitative agreement between theory and experiment also suggests that interactions within the monolayer may not significantly influence the measured transport properties. In transport measurements of densely packed monolayers, it is always possible that favorable transport pathways exist where current flows through multiple molecules connected by "through-space"[69] interactions in the monolayer. Recently, it was suggested that intermolecular interactions influenced the transport properties of alkanethiol monolayers on the basis of simulated inelastic electron tunneling spectra.[70] In molecules such as AQ and AH, where the coupling between large conjugated units is disrupted by small elements in the central part of the anthracene, it is plausible that current could flow through the monolayer by tunneling from one side of one molecule to the other side of a neighbor, possibly with similar ease to passing through a single molecule if π-stacking interactions were significant. While this scenario cannot be ruled out on the basis of these experiments, the qualitative agreement with single molecule transport calculations would tend to suggest that "through-bond" transport dominates.

CONCLUSIONS

EGaIn is a new tool for making conformal, nondamaging contacts to SAMs for electrical measurements. We have, for the first time, demonstrated that it can be used as a top-contact for tunneling junctions comprising SAMs of conjugated molecules and that, despite the (as of yet) poorly defined EGaIn|Ga_2O_3//SAM interface, we can differentiate molecules with broken-conjugation, cross-conjugation, and linear-conjugation even though they are of approximately the same length. We calculated the transport properties of these molecules, and although the poorly defined interface prevented quantitative comparisons, the calculations and data agree qualitatively: AC (linear-conjugation) is significantly more conductive than AQ (cross-conjugated) and AH (broken-conjugation). Ongoing studies using AC, AQ, and AH in single-molecule junctions as well as detailed studies of the influence of the Ga_2O_3 layer will help to eliminate any remaining ambiguities that prevent such quantitative comparisons. Nonetheless, these unambiguous results are the first experimental evidence for the existence of quantum interference effects in tunneling junctions comprising SAMs and extend the demonstrable usefulness of EGaIn for ME to include conjugated systems. While we were able to easily and rapidly collect statistically significant amounts of data on (chemically) fragile SAMs under ambient conditions, the data appear to be limited by the conductivity of the EGaIn|Ga_2O_3//SAM interface. This limit is evident in the histograms of log|J|, which are truncated at ~10 A/cm^2 at 0.4 V, a value for J_0 that has been estimated by two other studies of EGaIn tunneling junctions.[44,45] Gaussian fits of these histograms predict mean values of J that are higher than the maximum measured (and average) values of J but agree perfectly with the values predicted by our transport calculations. The electronic properties of the EGaIn|Ga_2O_3//SAM interface (and J_0 in particular) are expected to be dominated by the head-groups of the SAM, in this case a mixture of thiols and acetylthioaltes. These results highlight the importance of the Ga_2O_3 layer in EGaIn measurements; it simultaneously enables the simple, rapid measurement of myriad different types of SAMs on different substrates but limits the conductivity of the molecules that can currently be measured. We and others are investigating the influence of head-groups on J_0 in conjugated and nonconjugated systems in an effort to further extend the usefulness of EGaIn as a tool for ME.

ASSOCIATED CONTENT

Supporting Information. Experimental section, examples of raw and pruned J/V traces, histograms, and a detailed description of the EGaIn experimental setup and the formation of EGaIn tips, XPS and ellipsometry data, and the complete list of authors for ref 62. This material is available free of charge via the Internet at http://pubs.acs.org.

AUTHOR INFORMATION

Corresponding Author
gsolomon@nano.ku.dk; r.c.chiechi@rug.nl

ACKNOWLEDGMENT

G.C.S.'s research leading to these results has received funding from the European Research Council under the European Union's Seventh Framework Programme (FP7/2007-2013)/ERC Grant agreement no. 258806. H.V. acknowledges NanoNed, funded by the Dutch Ministry of Economic Affairs, for financial support (project GMM.6973). We thank Reinder Gooijaarts for technical support and the construction of the EGaIn measurement apparatus.

REFERENCES

(1) French, S. J.; Saunders, D. J.; Ingle, G. W. *J. Phys. Chem.* **1938**, *42*, 265–274.
(2) Gholami, M.; Tykwinski, R. R. *Chem. Rev.* **2006**, *106*, 4997–5027.
(3) Chiechi, R. C.; Sonmez, G.; Wudl, F. *Adv. Funct. Mater.* **2005**, *15*, 427–432.
(4) Sautet, P.; Joachim, C. *Chem. Phys. Lett.* **1988**, *153*, 511–516.
(5) Patoux, C.; Coudret, C.; Launay, J.-P.; Joachim, C.; Gourdon, A. *Inorg. Chem.* **1997**, *36*, 5037–5049.
(6) Yaliraki, S. N.; Ratner, M. A. *Ann. N.Y. Acad. Sci.* **2002**, *960*, 153–162.
(7) Hettler, M. H.; Wenzel, W.; Wegewijs, M. R.; Schoeller, H. *Phys. Rev. Lett.* **2003**, *90*, 076805.
(8) Stadler, R.; Ami, S.; Joachim, C.; Forshaw, M. *Nanotechnology* **2004**, *15*, S115–S121.
(9) Walter, D.; Neuhauser, D.; Baer, R. *Chem. Phys.* **2004**, *299*, 139–145.
(10) Cardamone, D. M.; Stafford, C. A.; Mazumdar, S. *Nano Lett.* **2006**, *6*, 2422–2426.
(11) Stafford, C. A.; Cardamone, D. M.; Mazumdar, S. *Nanotechnology* **2007**, *18*, 424014.
(12) Ke, S.-H.; Yang, W.; Baranger, H. U. *Nano Lett.* **2008**, *8*, 3257–3261.
(13) Solomon, G. C.; Andrews, D. Q.; Van Duyne, R. P.; Ratner, M. A. *ChemPhysChem* **2009**, *10*, 257–264.
(14) Hansen, T.; Solomon, G. C.; Andrews, D. Q.; Ratner, M. A. *J. Chem. Phys.* **2009**, *131*, 194704.
(15) Kocherzhenko, A. A.; Grozema, F. C.; Siebbeles, L. D. A. *J. Phys. Chem.* **2010**, *114*, 7973–7979.
(16) Mayor, M.; Weber, H. B.; Reichert, J.; Elbing, M.; von Hänisch, C.; Beckmann, D.; Fischer, M. *Angew. Chem.* **2003**, *42*, 5834–5838.

(17) Kiguchi, M.; Nakamura, H.; Takahashi, Y.; Takahashi, T.; Ohto, T. *J. Phys. Chem. C* **2010**, *114*, 22254–22261.
(18) Hush, N. S.; Reimers, J. R.; Hall, L. E.; Johnston, L. A.; Crossley, M. J. *Ann. N.Y. Acad. Sci.* **1998**, *852*, 1–21.
(19) Markussen, T.; Schiötz, J.; Thygesen, K. S. *J. Chem. Phys.* **2010**, *132*, 224104.
(20) Solomon, G. C.; Andrews, D. Q.; Van Duyne, R. P.; Ratner, M. A. *J. Am. Chem. Soc.* **2008**, *130*, 7788–7789.
(21) Solomon, G. C.; Andrews, D. Q.; Hansen, T.; Goldsmith, R. H.; Wasielewski, M. R.; Van Duyne, R. P.; Ratner, M. A. *J. Chem. Phys.* **2008**, *129*, 054701–8.
(22) Markussen, T.; Stadler, R.; Thygesen, K. S. *Nano Lett.* **2010**, *10*, 4260–4265.
(23) van Dijk, E. H.; Myles, D. J. T.; van der Veen, M. H.; Hummelen, J. C. *Org. Lett.* **2006**, *8*, 2333–2336.
(24) Ricks, A. B.; Solomon, G. C.; Colvin, M. T.; Scott, A. M.; Chen, K.; Ratner, M. A.; Wasielewski, M. R. *J. Am. Chem. Soc.* **2010**, *132*, 15427–15434.
(25) Dulić, D.; van der Molen, S. J.; Kudernac, T.; Jonkman, H. T.; de Jong, J. J. D.; Bowden, T. N.; van Esch, J.; Feringa, B. L.; van Wees, B. J. *Phys. Rev. Lett.* **2003**, *91*, 207402.
(26) Akkerman, H. B.; de Boer, B. *J. Phys.: Condens. Matter* **2007**, *20*, 013001–013021.
(27) Bumm, L. A. *ACS Nano* **2008**, *2*, 403–407.
(28) Engelkes, V. B.; Beebe, J. M.; Frisbie, C. D. *J. Am. Chem. Soc.* **2004**, *126*, 14287–14296.
(29) Wold, D.; Frisbie, C. *J. Am. Chem. Soc.* **2001**, *123*, 5549–5556.
(30) Mishchenko, A.; Vonlanthen, D.; Meded, V.; Bürkle, M.; Li, C.; Pobelov, I. V.; Bagrets, A.; Viljas, J. K.; Pauly, F.; Evers, F.; Mayor, M.; Wandlowski, T. *Nano Lett.* **2010**, *10*, 156–163.
(31) Xu, B.; Tao, N. J. *Science* **2003**, *301*, 1221–1223.
(32) With CP-AFM and STM-BJs the probe is rigid rather than conformal and can be pushed through the SAM, and thus the molecules are not defining the smallest dimension.
(33) Haag, R.; Rampi, M. A.; Holmlin, R. E.; Whitesides, G. M. *J. Am. Chem. Soc.* **1999**, *121*, 7895–7906.
(34) Holmlin, R. E.; Haag, R.; Chabinyc, M. L.; Ismagilov, R. F.; Cohen, A. E.; Terfort, A.; Rampi, M. A.; Whitesides, G. M. *J. Am. Chem. Soc.* **2001**, *123*, 5075–5085.
(35) Simeone, F. C.; Rampi, M. A. *CHIMIA* **2010**, *64*, 362–369.
(36) Slowinski, K.; Fong, H. K. Y.; Majda, M. *J. Am. Chem. Soc.* **1999**, *121*, 7257–7261.
(37) Slowinski, K.; Chamberlain, R. V.; Miller, C. J.; Majda, M. *J. Am. Chem. Soc.* **1997**, *119*, 11910–11919.
(38) York, R.; Nacionales, D.; Slowinski, K. *Chem. Phys.* **2005**, 235–242.
(39) York, R. L.; Nguyen, P. T.; Slowinski, K. *J. Am. Chem. Soc.* **2003**, *125*, 5948–5953.
(40) Dickey, M. D.; Chiechi, R. C.; Larsen, R. J.; Weiss, E. A.; Weitz, D. A.; Whitesides, G. M. *Adv. Funct. Mater.* **2008**, *18*, 1097–1104.
(41) Dumke, M.; Tombrello, T.; Weller, R.; Housley, R.; Cirlin, E. *Surf. Sci.* **1983**, *124*, 407–422.
(42) Nijhuis, C. A.; Reus, W. F.; Barber, J. R.; Dickey, M. D.; Whitesides, G. M. *Nano Lett.* **2010**, *10*, 3611–3619.
(43) Siegel, A. C.; Tang, S. K. Y.; Nijhuis, C. A.; Hashimoto, M.; Phillips, S. T.; Dickey, M. D.; Whitesides, G. M. *Acc. Chem. Res.* **2010**, *43*, 518–528.
(44) Thuo, M. M.; Reus, W. F.; Nijhuis, C. A.; Barber, J. R.; Kim, C.; Schulz, M. D.; Whitesides, G. M. *J. Am. Chem. Soc.* **2011**, *133*, 2962–2975.
(45) Nijhuis, C. A.; Reus, W. F.; Whitesides, G. M. *J. Am. Chem. Soc.* **2009**, *131*, 17814–17827.
(46) Chiechi, R. C.; Weiss, E. A.; Dickey, M. D.; Whitesides, G. M. *Angew. Chem.* **2008**, *47*, 142–144.
(47) Grave, C.; Risko, C.; Shaporenko, A.; Wang, Y.; Nuckolls, C.; Ratner, M. A.; Rampi, M. A.; Zharnikov, M. *Adv. Funct. Mater.* **2007**, *17*, 3816–3828.
(48) Valkenier, H.; Guédon, C. M.; Markussen, T.; Thygesen, K. S.; van der Molen, S. J.; Hummelen, J. C. Manuscript in preparation.
(49) Milani, F.; Grave, C.; Ferri, V.; Samor, P.; Rampi, M. A. *Chem. Phys. Chem.* **2007**, *8*, 515–518.
(50) Akkerman, H. B.; Blom, P. W. M.; de Leeuw, D. M.; de Boer, B. *Nature* **2006**, *441*, 69–72.
(51) Kronemeijer, A. J.; Huisman, E. H.; Akkerman, H. B.; Goossens, A. M.; Katsouras, I.; van Hal, P. A.; Geuns, T. C. T.; van der Molen, S. J.; Blom, P. W. M.; de Leeuw, D. M. *Appl. Phys. Lett.* **2010**, *97*, 173302–173302−3.
(52) Kronemeijer, A. J.; Huisman, E. H.; Katsouras, I.; van Hal, P. A.; Geuns, T. C. T.; Blom, P. W. M.; van der Molen, S. J.; de Leeuw, D. M. *Phys. Rev. Lett.* **2010**, *105*, 156604.
(53) Lorenz, M.; Woods, J.; Gambino, R. *J. Phys. Chem.* **1967**, *28*, 403–404.
(54) Nijhuis, C. A.; Reus, W. F.; Whitesides, G. M. *J. Am. Chem. Soc.* **2010**, *132*, 18386–18401.
(55) Weiss, E. A.; Kaufman, G. K.; Kriebel, J. K.; Li, Z.; Schalek, R.; Whitesides, G. M. *Langmuir* **2007**, *23*, 9686–9694.
(56) Weiss, E. A.; Chiechi, R. C.; Kaufman, G. K.; Kriebel, J. K.; Li, Z.; Duati, M.; Rampi, M. A.; Whitesides, G. M. *J. Am. Chem. Soc.* **2007**, *129*, 4336–4349.
(57) Engelkes, V. B.; Beebe, J. M.; Frisbie, C. D. *J. Phys. Chem. B* **2005**, *109*, 16801–16810.
(58) DeRose, J. A.; Thundat, T.; Nagahara, L. A.; Lindsay, S. M. *Surf. Sci.* **1991**, *256*, 102–108.
(59) Porath, D.; Goldstein, Y.; Grayevsky, A.; Millo, O. *Surf. Sci.* **1994**, *321*, 81–88.
(60) We never observe $I = 0$ A but define the value with the electrodes disconnected ($<10^{-15}$ A) as zero.
(61) Valkenier, H.; Huisman, E. H.; van Hal, P. A.; de Leeuw, D. M.; Chiechi, R. C.; Hummelen, J. C. *J. Am. Chem. Soc.* **2011**, *133*, 4930–4939.
(62) Shao, Y.; et al. *Phys. Chem. Chem. Phys.* **2006**, *8*, 3172–3191.
(63) Bilic, A.; Reimers, J. R.; Hush, N. S. *J. Chem. Phys.* **2005**, *122*, 094708–15.
(64) Elstner, M.; Porezag, D.; Jugnickel, G.; Elsner, J.; Haugk, M.; Frauenheim, T.; Suhai, S.; Seifert, G. *Phys. Rev. B* **1998**, *58*, 7260–7268.
(65) Frauenheim, T.; Seifert, G.; Elstner, M.; Hagnal, Z.; Jungnickel, G.; Porezag, D.; Suhai, S.; Scholz, R. *Phys. Status Solidi B* **2000**, *217*, 41–62.
(66) Frauenheim, T.; Seifert, G.; Elstner, M.; Niehaus, T.; Koehler, C.; Amkreutz, M.; Sternberg, M.; Hajnal, Z.; Di Carlo, A.; Suhai, S. *J. Phys.: Condens. Matter* **2002**, *14*, 3015–3047.
(67) Porezag, D.; Frauenheim, T.; Kohler, T.; Seifert, G.; Kaschner, R. *Phys. Rev. B* **1995**, *51*, 12947–12957.
(68) Pecchia, A.; Di Carlo, A. *Rep. Prog. Phys.* **2004**, *67*, 1497–1561.
(69) Hoffmann, R. *Acc. Chem. Res.* **1971**, *4*, 1–9.
(70) Okabayashi, N.; Paulsson, M.; Ueba, H.; Konda, Y.; Komeda, T. *Phys. Rev. Lett.* **2010**, *104*, 077801.